Neuron, Vol. 40, 41–52, September 25, 2003, Copyright ©2003 by Cell Press

Neuropathogenic Forms of Huntingtin and Androgen Receptor Inhibit Fast Axonal Transport

György Szebenyi,[1,8,9] Gerardo A. Morfini,[3,4,8] Alyssa Babcock,[4] Milena Gould,[4] Kimberly Selkoe,[4] David L. Stenoien,[1,4] Maureen Young,[2] Pieter W. Faber,[5,6,10] Marcy E. MacDonald,[5,7] Michael J. McPhaul,[2] and Scott T. Brady[3,4,*]

[1]Department of Cell Biology
[2]Department of Internal Medicine
University of Texas Southwestern Medical Center
Dallas, Texas 75390
[3]Department of Anatomy and Cell Biology
University of Illinois at Chicago
Chicago, Illinois 60612
[4]Marine Biological Laboratory
Woods Hole, Massachusetts 02543
[5]Molecular Neurogenetics Unit
[6]Cancer Center
[7]Laboratory for Molecular Neuropathology
Massachusetts General Hospital
Charlestown, Massachusetts 02129

Summary

Huntington's and Kennedy's disease are autosomal dominant neurodegenerative diseases caused by pathogenic expansion of polyglutamine tracts. Expansion of glutamine repeats must in some way confer a gain of pathological function that disrupts an essential cellular process and leads to loss of affected neurons. Association of huntingtin with vesicular structures raised the possibility that axonal transport might be altered. Here we show that polypeptides containing expanded polyglutamine tracts, but not normal N-terminal huntingtin or androgen receptor, directly inhibit both fast axonal transport in isolated axoplasm and elongation of neuritic processes in intact cells. Effects were greater with truncated polypeptides and occurred without detectable morphological aggregates.

Introduction

Understanding pathogenic mechanisms is essential for devising effective treatments for neurodegenerative diseases. Glutamine repeat expansion diseases include Huntington's disease (HD), Kennedy's disease or Spinobulbar Muscular Atrophy (SBMA), Dentatorubral-Pallidoluysian Atrophy, and Spinocerebellar Ataxias (SCA types 1, 2, 3, 6, and 7) (Fischbeck, 2001; Gusella and MacDonald, 2000; Zoghbi and Orr, 2000). In each case, disease results from increases in the number of residues in a polyglutamine (polyQ) tract, ranging from normal lengths of 20–25 glutamines to pathological expansions of >40. Neurological symptoms typically appear in midlife, although longer polyQ repeats are associated with earlier onset of symptoms. Aside from the polyQ tracts, gene products associated with polyQ diseases exhibit minimal sequence homology. Knockouts of genes encoding polyQ-containing proteins result in different phenotypes, whereas expansion of polyQ tracts in each leads to a similar gain-of-function abnormality, albeit in distinct cell populations with a different clinical presentation. Indeed, introducing a polyQ stretch to a housekeeping protein hypoxanthine phosphoribosyltransferase in mouse produces neuropathology (Ordway et al., 1997), as does expression of truncated disease gene products containing expanded polyglutamine segments in cell and mouse systems (Gusella and MacDonald, 2000). This suggests that expansion of polyQ segments is sufficient to produce neurodegenerative disease. However, the gain of function conferred by polyQ expansion is unknown. Similarly, reasons for late onset of symptoms and increased susceptibilities of certain neuronal populations in these diseases are poorly understood, although the latter must be determined by the protein context in which polyglutamine expansion is presented to specific neuronal populations (Gusella and MacDonald, 2000; Orr, 2001).

Various mechanisms have been proposed for neuronal degeneration in polyQ diseases (Hughes and Olson, 2001; Rubinsztein, 2002). Altered neuronal energy metabolism was reported in HD, but these changes may be secondary to pathology and do not explain selective neuronal vulnerability. Excitotoxicity was also proposed to play a role in neuronal loss, but many neuronal populations sensitive to excitotoxicity are not primary targets in these diseases. Discovery of intranuclear inclusions in neurons of HD patients led to suggestions that these deposits might cause neuronal death. However, studies on animal and cellular models indicate that formation of nuclear and cytoplasmic inclusions correlates poorly with neuronal death and may be protective in some cases (Emamian et al., 2003; Orr, 2001; Rubinsztein, 2002), leaving open the question of whether nuclear localization and aggregation are required for pathogenesis. Regardless, molecular mechanisms by which aggregate formation or altered protein structures associated with polyglutamine expansions compromise neuronal function and lead to neuronal death are not apparent. Evidence that critical neuronal pathways are altered is seen in reports that SCA1 phosphorylation plays an important role in pathogenesis of SCA1 mice (Chen et al., 2003; Emamian et al., 2003). Regardless, one or more cellular component essential to neuronal function must be altered pathologically to trigger neuronal degeneration.

Cytoplasmic localization and association with vesicular structures for several pathogenic polyQ proteins raised the possibility that these proteins might interfere with normal trafficking of vesicles in fast axonal transport. Most pathogenic polyQ-containing proteins can be found in both nucleus and cytoplasm (Reddy et al.,

*Correspondence: stbrady@uic.edu
[8]These authors contributed equally to this work.
[9]Present address: Center for Basic Neuroscience, UT Southwestern, Dallas, Texas 75390.
[10]Present address: Athersys, Inc., Cleveland Functional Genomics, Cleveland, Ohio 44115.

1999), whereas SCA2 is localized exclusively in cytoplasm (Huynh et al., 2000). Although present in nuclei, huntingtin is predominantly cytoplasmic where it may be associated with vesicles or cytoskeletal structures (DiFiglia et al., 1995; Trettel et al., 2000; Trottier et al., 1995; Velier et al., 1998). Huntingtin is also moved in fast axonal transport (Block-Galarza et al., 1997), consistent with vesicle association. To determine whether normal or pathogenic polyQ-containing polypeptides affect vesicle transport in neurons, recombinant N-terminal huntingtin fragments were perfused into isolated axoplasm from squid giant axons, and effects on fast axonal transport were assessed under conditions with no detectable aggregates or nuclei. Only pathogenic forms inhibited vesicle transport. The effects of huntingtin raised the question of whether inhibition of transport was a general characteristic of expanded polyglutamine segments or unique to truncated huntingtin polypeptides. To test whether other proteins with pathological polyglutamine expansions inhibited axonal transport, effects on transport of full-length and truncated androgen receptors with normal or pathogenic length polyglutamine tracts were evaluated in isolated axoplasm and transport-dependent events in cultured cells.

Results

Recombinant Huntingtin Fragment with PolyQ Expansion Inhibits Fast Axonal Transport in Isolated Axoplasm

To assess effects on transport, polypeptides comprising amino acids (aa) 1–548 of human huntingtin (HD548) with 2, 23, 62, or 100 Qs were expressed by in vitro translation. Recombinant polypeptides included either N terminus FLAG or C terminus Green Fluorescent Protein (GFP) epitope tags (Figure 1A). Nonpathogenic (HD548-Q2 and -Q23) and pathogenic (HD548-Q62 and -Q100) length polypeptides were perfused into axoplasm extruded from giant axons of the squid *Loligo pealii* (Brady et al., 1985). Final concentration of recombinant huntingtin in axoplasm was typically 0.1–0.2 nM. By comparison, kinesin concentration in squid axoplasm is $\approx$0.5 μM (Brady et al., 1990; Stenoien and Brady, 1997) and tubulin is 50 μM (Morris and Lasek, 1984).

When control buffers or N-terminal huntingtin polypeptides containing 2 or 23 glutamines were perfused into axoplasm, fast axonal transport in both anterograde and retrograde directions continued unchanged for $\geq$1 hr (Figure 1B). In contrast, perfusion with huntingtin containing expanded polyQ tracts (Q62 or Q100) reduced mean transport velocities in both anterograde and retrograde directions by $>$50% within 50 min (Figure 1C). Significant declines in transport rates were evident within 25–35 min of perfusion. Reduced rates were accompanied by substantial reductions in amounts of vesicle traffic both in the axoplasm interior (Figure 1C) and on isolated microtubules at axoplasmic edges (not shown). Comparisons of transport rates between axoplasms perfused with different N-terminal huntingtin polypeptides (Figure 1D) show that reductions occurred only with expanded polyQ polypeptides (HD548-Q62flag, -Q100flag [not shown], and -Q62GFP). Vesicle movements in axoplasms perfused with polypeptides containing shorter polyQ tracts (HD548-Q2flag, -Q23flag, and -Q23GFP) were indistinguishable from empty pcDNA controls. Therefore, only N-terminal huntingtin polypeptide fragments containing polyQ segments in the disease-associated range disrupt fast axonal transport.

Wild-type, full-length huntingtin is associated with cytoplasmic vesicles (DiFiglia et al., 1995; Sharp et al., 1995), a subcellular location consistent with effects on vesicle transport. To see whether recombinant polypeptides comprising the huntingtin N-terminal 548 aa with various polyQ lengths were comparably localized in axoplasm, preparations perfused with HD548-Q23flag or HD548-Q62flag were immunolabeled with antiFLAG antibodies (Figure 1E). Staining patterns obtained for HD548-Q23 and HD548-Q62 were indistinguishable in multiple images from multiple axoplasms prepared by two fixation protocols (formaldehyde, Figure 1E; and alcohol/acid, not shown) and probed with two different anti-FLAG antibodies (M2, Figure 1E; and M5, not shown). Immunoreactivity appeared as small punctate structures reminiscent of patterns obtained in isolated axoplasm with antibodies against kinesin heavy or light chains (Brady et al., 1990; Stenoien and Brady, 1997). Kinesin in these preparations is almost entirely associated with membrane bounded organelles (Tsai et al., 2000). Given the association of huntingtin with vesicular structures in vivo (DiFiglia et al., 1995; Sharp et al., 1995), these puncta are likely to represent axoplasmic vesicles. No evidence of aggregate formation was seen with either HD548-Q23flag or -Q62flag N-terminal huntingtin polypeptides. This suggests that huntingtin N terminus is sufficient for localization to vesicular structures and that expansion of polyQ tracts does not interfere with localization. Therefore, pathogenic polyQ-containing N-terminal huntingtin polypeptides inhibited axonal transport without any apparent change in distribution patterns.

SBMA-Associated Forms of PolyQ Androgen Receptor Attenuate Morphological Differentiation of Neuronal Cell Lines

To determine whether inhibition of axonal transport was unique to N-terminal huntingtin fragments with polyQ expansion or a general characteristic of proteins with polyQ expansion, SH-SY5Y human neuroblastoma cells were stably transfected with androgen receptor (AR) constructs containing wild-type Q20 and pathogenic (SBMA) Q56 tracts. Untransfected SH-SY5Y cells contain very low levels of endogenous AR (Grierson et al., 2001). Position of the AR polyQ stretch is illustrated in Figure 2A. Stably transfected cell lines were selected for moderate expression levels (see Figures 2B–2D) to avoid artifacts associated with overexpression of recombinant polypeptides (Szebenyi et al., 2002). Three transfected clones were selected for further characterization: wtAR with full-length AR-Q20, 902-13 with full length AR-Q56, and 902-6 with both full-length AR-Q56 and a spontaneously generated polyQ AR N-terminal fragment (Figure 2B). The AR N-terminal fragment reacted with antibodies recognizing aa 1–20 of the AR, U402 (Figure 2B) and N20 (Figure 2E), but not with 441

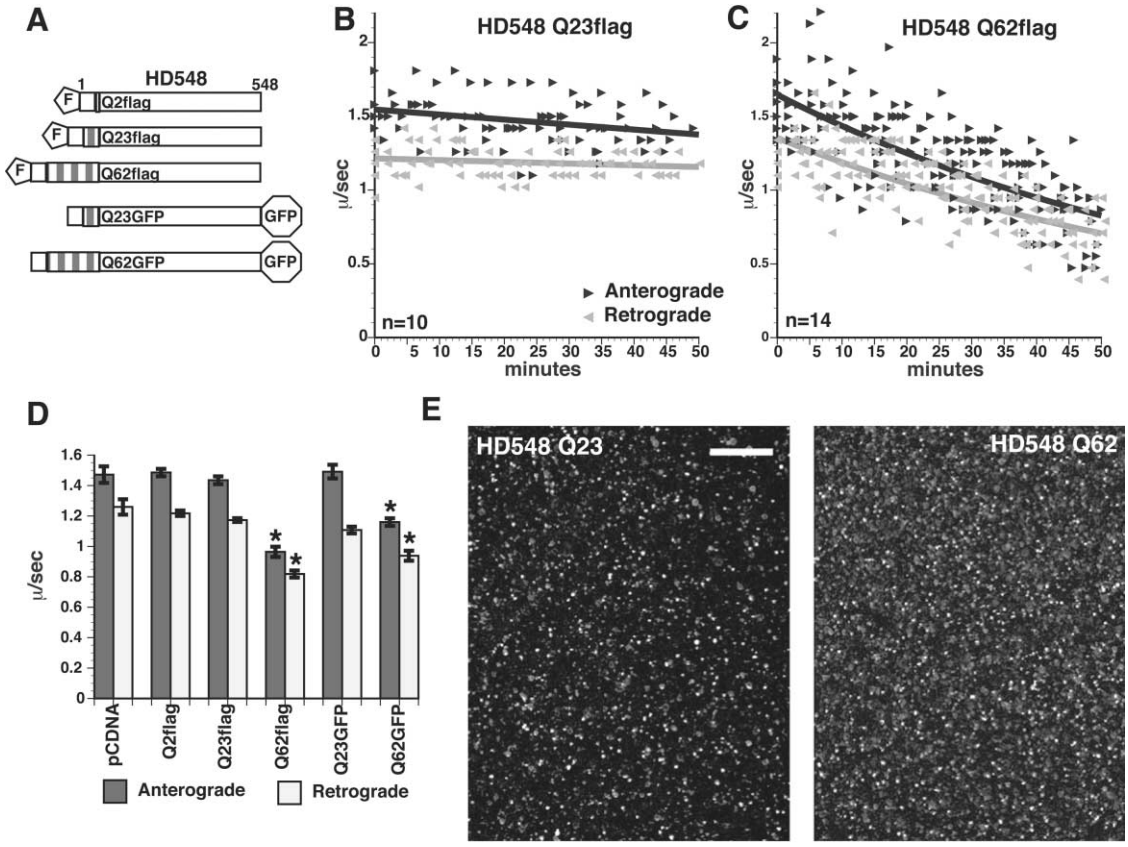

Figure 1. Pathogenic Forms of Recombinant Huntingtin Inhibit Fast Axonal Transport in Isolated Axoplasm

(A) Expression vectors encoding amino acids 1–548 of human huntingtin (HD548) with 2 and 23 (nonpathogenic) and 62 and 100 (pathogenic) Qs were constructed and polypeptides synthesized by in vitro translation. Constructs either had a FLAG epitope tag at their N terminus or Green Fluorescent Protein (GFP) at their C terminus.

(B) Perfusion of 0.1–0.2 nM HD548-Q23flag had no effect on fast axonal transport in either anterograde or retrograde direction over 50 min.

(C) Perfusion of HD548-Q62flag at concentrations comparable to HD548-Q23flag resulted in a time-dependent reduction of >50% over 50 min in the mean velocity of vesicles moving in fast axonal transport, both anterograde and retrograde.

(D) Histograms comparing actions of pathogenic and nonpathogenic polypeptides on fast axonal transport after 25–35 min of observation. Fast axonal transport in the presence of nonpathogenic polypeptides was indistinguishable from vector controls (pCDNA) or unperfused axoplasm (data not shown). In contrast, fast axonal transport was significantly reduced (*$p \leq 0.001$ in a pooled t test) by polypeptides containing pathogenic numbers of glutamines.

(E) By immunofluorescence, both pathogenic and nonpathogenic HD548 perfused into axoplasm appear as small punctate structures. No evidence of aggregate formation was seen for either HD548-Q62flag or HD548-Q23flag peptides. Results of staining with M2 antiFLAG antibody are shown. Scale bar equals 2.0 μm.

antibody against aa 299–315 (Figure 2C) or U407 antibody against aa 200–220 (numbering as in wt AR-Q20) (not shown) on immunoblots. Staining with 1C2, an antibody that binds to polyQ tracts containing ≥20 glutamines (Perez et al., 1999; Trottier et al., 1995), confirmed that the small AR fragment included a polyQ segment (Figure 2E, middle panel). Cells expressed full-length wild-type AR at approximately 7 times the level of the two mutant cell lines (902-6 and 902-13) (Figure 2D).

Subcellular location of polyQ-AR proteins was examined by immunoblotting of subcellular fractions (Figure 2E) and immunofluorescence of fixed cells (Figures 2F–2H). Immunoblots of subcellular fractions from each cell line showed enrichment of small polyQ AR fragment in soluble cytoplasmic fractions (Figure 2E). Full-length AR (both wild-type and pathogenic) was enriched in membrane fractions, similar to apparent localization of N-terminal huntingtin on vesicles in axoplasm (Figure 1E). Recombinant AR was seen by immunofluorescence in both nucleus and cytoplasm of all three cell lines (Figures 2F–2H), with immunoreactivity concentrated in nuclei of a subset of cells. Although expression levels and relative subcellular distributions of AR varied between cells within the same culture, immunostaining levels with antibodies against AR N-terminal (Figure 2F, N20) were consistently higher in 902-6 cells than in wild-type or 902-13 cells. Staining intensities with antibodies against AR C-terminal epitopes not present in the fragment were comparable (Figure 2F, 441). Significantly, there was no evidence of morphologic aggregates in either cytoplasm or nucleus in any of the cell lines despite examination of hundreds of cells under the microscope and in digital images. These observations suggest that the fragment was stable and accumulated in cells comparably in nuclear and cytoplasmic compartments. Under these culture conditions, no aggregates of

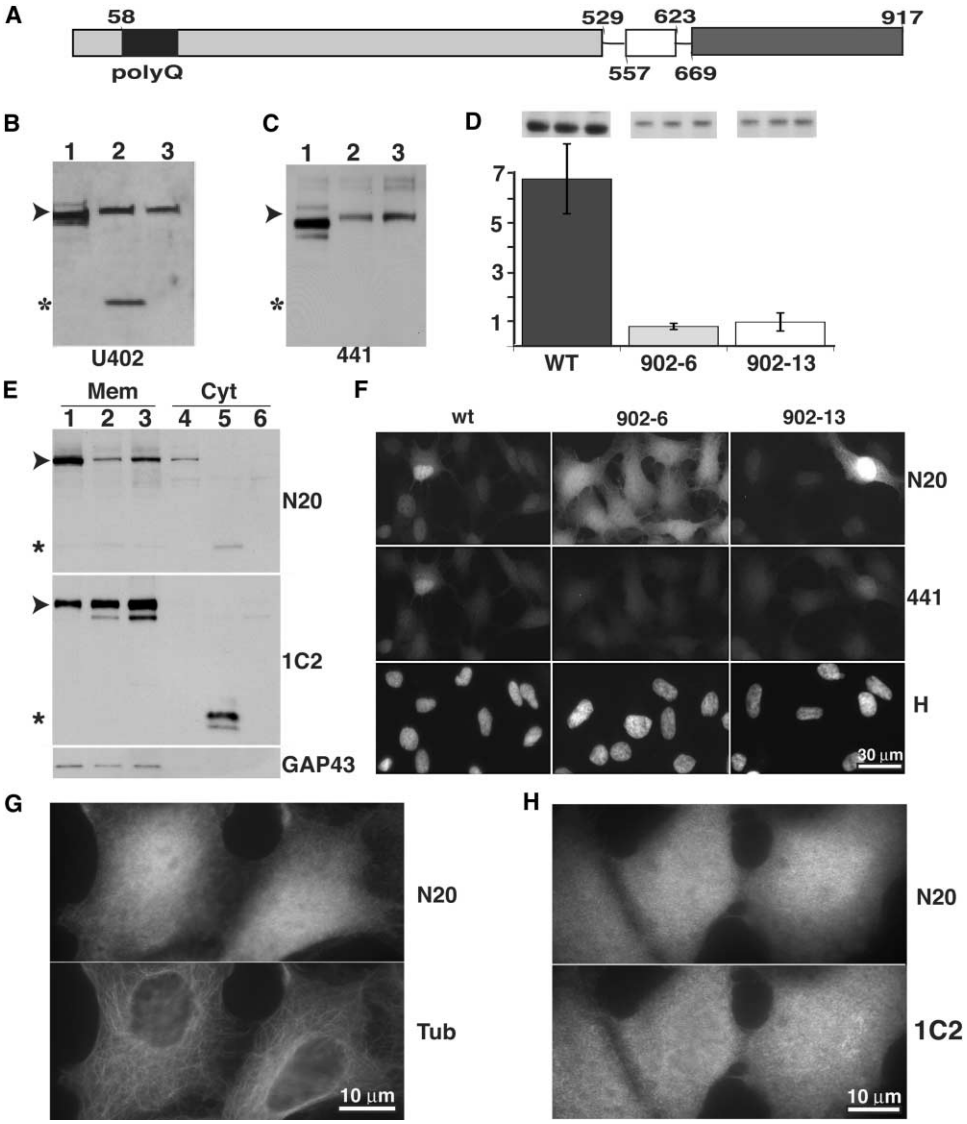

Figure 2. A Truncated PolyQ Containing AR N-Fragment Accumulates in AR-Q56 Transfected SH-SY5Y Cell Cytoplasm

(A) Schematic showing domain organization of human AR: sequence locations for carboxyl hormone binding (aa 669–917; dark gray), DNA binding (aa 557–623; white), and amino-terminal transactivation domains (aa 1–529; light gray) are indicated. A polyglutamine tract near the N terminus (black box, starting at aa 58) contains Q20 in wtAR, and Q56 in 902-6 and 902-13 stably transfected clones of SH-SY5Y cells.

(B) Immunoblot with U402 antibody (against AR aa 1–20) of cell lysates of wtAR (1), 902-6 (2), or 902-13 (3). Wild-type AR-Q20 is expressed at higher levels and, as expected, runs at a lower MW (≈110 kDa, arrow) than AR-Q56 in 902-6 and 902-13 clonal lines. In 902-6 cells, an additional band (*) is seen at MW ≈25 KD.

(C) Immunoblot of cell lysates with 441 antibody (AR aa 299–315, Santa Cruz) shows reactivity with full-length AR but not with the polyQ-containing AR N-terminal fragment in 902-6 cells. Symbols are as in (B).

(D) Quantitation of full-length AR in the three cell lines. Cultures were done in triplicate for each cell line and gels loaded at constant total protein. Bars show relative band intensities normalized to loading controls. The *y* axis is shown in arbitrary units. Standard deviations are indicated. AR is undetectable in nontransfected cells. Cells transfected with wtAR expressed 7 times as much AR as either cell line expressing mutant AR. Therefore, effects seen with mutant AR were due to the presence of mutations rather than expression artifacts.

(E) Immunoblots of microsomal (1–3) and cytosolic (4–6) fractions of wtAR (1 and 4), 902-6 (2 and 5), and 902-13 (3 and 6) cells with N20 antibody confirm that polyQ-AR is present in compartments outside the nucleus. Symbols are as in (B). Staining with 1C2 (Chemicon) antibody that reacts with polyQ tracts containing >20 Qs demonstrates presence of a polyQ stretch in both full-length AR and cytoplasmic N-terminal fragments. The membrane protein GAP-43 (Boehringer Mannheim) is not in cytosolic fractions.

(F) Cultures of wtAR, 902-6, and 902-13 were triple stained with N20 (AR aa 1–20, Santa Cruz) and 441 Abs and a nuclear-specific Hoechst (H) dye. Staining patterns and intensities are similar in each of the three cell lines with 441, whereas staining intensity with N20 in the 902-6 cells is much higher due to reaction with N-terminal fragment. In every cell line and with each anti-AR antibody, immunoreactivity was observed throughout the nucleus and cytoplasm.

(G) Higher magnification images of 902-6 cells double immunostained with N20 and DM1A (anti α-tubulin) show that polyQ-AR is found in both nuclear and cytoplasmic compartments.

(H) Double staining with N20 and 1C2 shows that epitopes recognized by these antibodies colocalize. Note absence of either cytoplasmic or nuclear aggregates with these antibodies.

polyQ-expanded polypeptides were apparent in either 902-6 or 902-13 cells.

Characteristics of cells harboring expanded polyQ AR-Q56 constructs (902-6 and 902-13) were compared to wtAR controls. After plating and growth in serum-containing medium, wtAR-transfected SH-SY5Y cells spread out in all directions. Upon serum withdrawal and BDNF addition, they developed polarized, elongated morphologies (Figure 3A, left column). By 25 days in culture (19 days postBDNF application), a network of neurites comparable to induced, untransfected SH-SY5Y cells (Encinas et al., 2000) was obvious. In contrast, 902-6 cultures appeared less differentiated at each time point (Figure 3A, right column). Morphological differences were obvious even 3 days after BDNF treatment, as shown by tubulin staining of fixed cultures (Figure 3B). Cell lengths were measured to quantitate differences. Results of parametric statistical analysis are shown in Table 1. Mean cell lengths for all three lines differed significantly ($p < 0.01$, Student's t test), with wtAR cells being longest and 902-6 cells shortest. Histograms in Figure 3B show percentages of cells within a given size range for each cell line. In wtAR, 30% of analyzed cells are <61 μm, while in 902-13 44% and in 902-6 66% of cells fell within this range. Conversely, 40% of wtAR cells are >81 μm, whereas only 15% of 902-13 and 8% of 902-6 cells are this long. Despite significant differences in both mean values and shapes of histograms, there was overlap in cell morphologies. Interestingly, double immunostaining of 902-6 cells for AR and tubulin showed that cells with more differentiated shapes had lower levels of polyQ-AR (Figure 3C, see Supplemental Figure S1 at http://www.neuron.org/cgi/content/full/40/1/41/DC1).

Changes in cell number after various treatments were monitored over time to determine if growth rates in serum-containing medium, growth arrest in response to retinoic acid and BDNF, or cell death after growth factor withdrawal differed between wt AR and 902-6 cells. 902-6 cells were selected because they had higher polyQ-AR immunoreactivity (Figure 2) and more severe morphological defects (Figure 3B). Mean values in cell numbers between cell lines (Figures 3D and 3E) showed comparable proliferation rates with serum (days 1–6), and both cell lines responded to BDNF in serum-free medium (day 6) by growth arrest (Figure 3D). Both wtAR and 902-6 cells exhibited significant loss of cells after BDNF removal (Figure 3E). Average cell numbers in 902-6 cultures were reduced relative to parallel wtAR cultures after growth factor washout in four independent experiments, but differences did not reach significance ($p = 0.1$ in Student's t test). Taken together, these data indicate that expression of expanded polyQ AR attenuates outgrowth of neurites without affecting other aspects of cell behavior.

Overall distribution of motor proteins is not altered in polyQ AR-expressing cells. A possible explanation for defective axonal transport in isolated axoplasm and transport-dependent neurite extension in polyQ AR-containing intact cells is that expansion of polyQ tracts alters motor protein distribution. To evaluate distributions of kinesin and dynein in intact cells, uninduced SH-SY5Y cells with and without transfection (Figure 4A) and BDNF-induced wtAR and 902-6 cells (Figure 4B) were immunostained. Staining was punctate in all cases for both kinesin and dynein. This distribution is consistent with previous studies showing that $\geq$95% cellular kinesin is membrane associated (Elluru et al., 1995; Tsai et al., 2000). Similarly, the 74.1 antibody used to localize dynein preferentially stains membrane-associated dynein in immunofluorescence (Li et al., 2000). BDNF induction of differentiation increased kinesin levels moderately. Presence of AR-Q56 did not dramatically alter distribution patterns for motors relative to wtAR cells, although slight increases in kinesin immunoreactivity were seen in the periphery of some 902-6-expressing cells. This distribution may result from the altered morphology of these cells or differences in cell motility.

Expanded PolyQ Forms of AR Inhibit Fast Axonal Transport in Isolated Axoplasm

As with N-terminal huntingtin polypeptides, perfusion with subnanomolar concentrations of in vitro translated full-length or N-terminal wild-type AR had no detectable effect on fast axonal transport in isolated axoplasm (Figures 5A, 5D, and 5F). In contrast, perfusion of comparable amounts of full-length or N-terminal expanded polyQ AR inhibited both directions of transport significantly (Figures 5B, 5E, and 5F). These effects were not associated with aggregate formation in expanded polyQ AR, because full-length AR with wild-type (20Q) and pathogenic (56Q) length polyglutamine tract behaved comparably in gel filtration chromatography (Figure 5C). Perfusion with full-length pathogenic AR affected anterograde transport more severely than retrograde, whereas effects of pathogenic AR N-terminal fragments (Figure 5E) resembled huntingtin N-terminal polypeptide effects. However, both full-length and N-terminal fragments significantly inhibited transport in both anterograde and retrograde directions ($p \leq 0.0001$). Fragments with expanded polyQ fragments affected both anterograde and retrograde transport more severely than full-length cognates (Figures 5B, 5E, and 5F), consistent with the more severe attenuation in neurite outgrowth in 902-6 cells relative to 902-13 cells (Figure 3 and Table 1). This differential effect may reflect differences in concentration of polyQ-containing polypeptide. In vitro translation methods typically produce more copies of shorter constructs, so N-terminal fragments may be present at higher concentration. Consistent with this, staining of 902-6 cells show increased levels of polyQ domains when truncated peptide is taken into account (see 1C2 and N20 staining in Figures 2F and 2H as compared to 441 staining in Figure 2F).

Consistent with observations that expanded polyQ AR inhibits transport of neuronal organelles, mitochondrial distribution was affected in a neuron-like cell line expressing high levels of an expanded polyQ mutant AR recombinant protein (Piccioni et al., 2002). However, transport defects do not result from inhibition of energy production by oxidative phosphorylation because perfusion buffer contains 5 mM ATP, which supports transport in the absence of mitochondrial function (Brady et al., 1985). This suggests that effects of expanded polyQ peptides on fast axonal transport are mediated through an action on microtubule motor function rather than on cellular energy supplies.

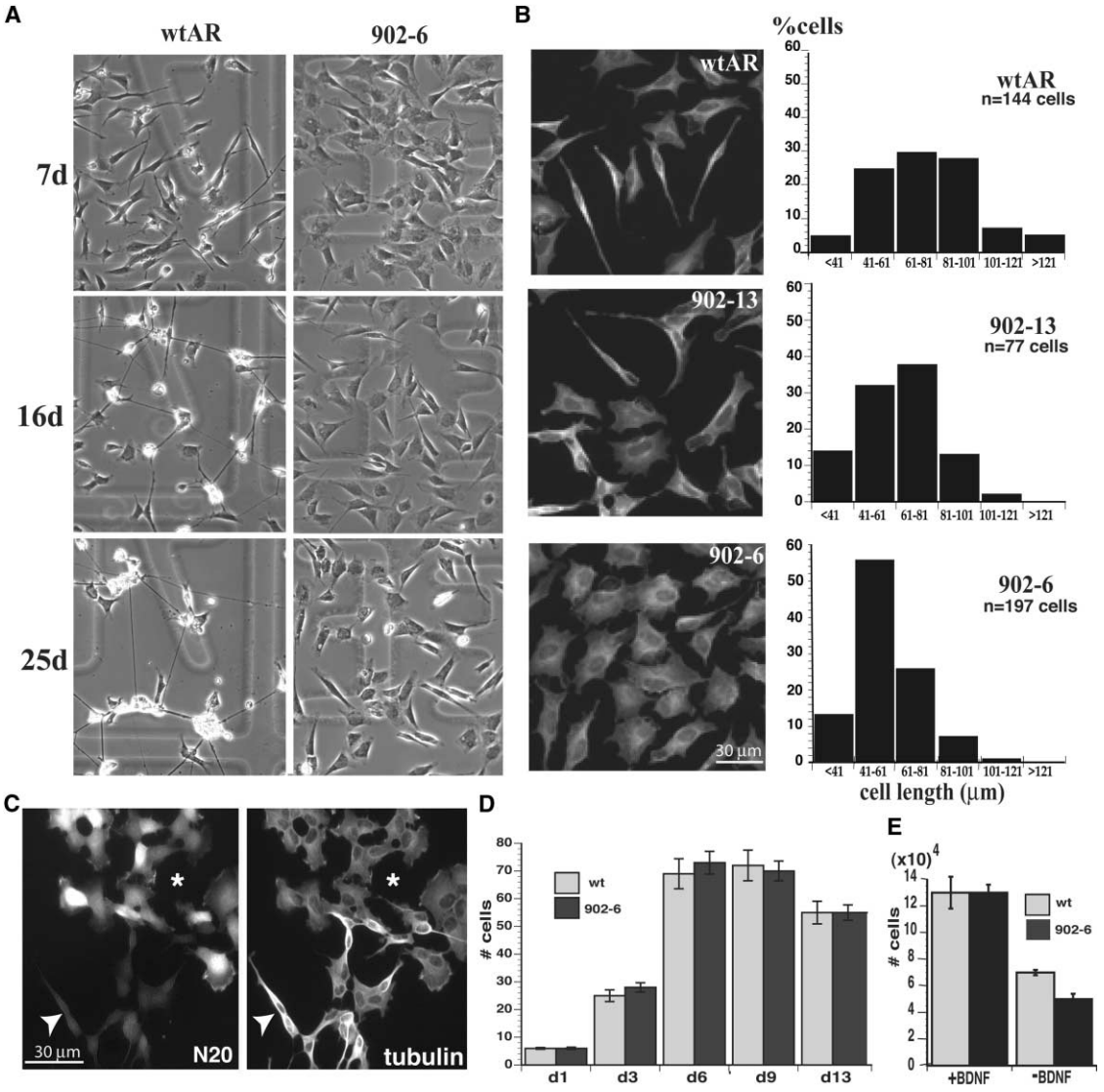

Figure 3. PolyQ-AR Inhibits Process Elongation in SH-SY5Y Cells

(A) Phase images of live wtAR and 902-6 cells at various times after plating. Differentiation was induced with BDNF on day 6. WtAR cells were more elongated than 902-6 cells at each time point and formed fasciculated networks of neuritic processes by 2 weeks.

(B) Cells immunostained for α-tubulin (DM1A, Sigma) are shown 3 days after BDNF treatment. Histograms show cell length distributions. Even at early times, most wtAR cells were elongated, whereas 902-6 cells were smaller and less polarized. 902-13 cells were intermediate in size between wtAR and 902-6 cells. Thus, presence of the small N-terminal fragment correlates with more pronounced phenotypic differences.

(C) In a given 902-6 cell culture, subpopulations of cells with phenotypes like wtAR could occasionally be seen. Comparison of AR (N20) and tubulin immunoreactivity indicates that more elongated, differentiated cells expressed much lower levels of polyQ-AR (arrow). Cells with intense AR staining (*) lacked polarity, indicating that presence of expanded polyQ domain inhibits process extension.

(D) Effects of expanded polyQ domains on proliferation and survival were evaluated by counting live cells in wtAR and 902-6 cultures in the corresponding areas of culture dishes defined by marks etched into coverslips. Results of a single experiment are shown. Error bars are SEM with n = 30 squares counted. Retinoic acid was added 1 day postplating and BDNF on day 6. Similar results were obtained in three independent experiments involving 66 squares on 7 dishes for each cell line and by cell counts of trypsinized cells in three independent experiments with a total of 8 plates for each time point (data not shown). There were no significant differences between cell lines in replication rates with serum-containing medium or growth arrest in response to BDNF in serum-free medium.

(E) To test sensitivity of wtAR and 902-6 cells to withdrawal of trophic factors, cell numbers in cultures grown for 3 days in BDNF (+BDNF) were compared to cell numbers remaining 2–3 days after growth factor washout (−BDNF). Hemocytometer cell counts following trypsinization are shown. Error bars are SEM with n = 5 plates for +BDNF for each cell line, and n = 10 for −BDNF. Qualitatively similar results were obtained by counting live cells in the same dish before and after BDNF washout (not shown).

Discussion

Inhibition of fast axonal transport provides a novel mechanism for polyQ pathogenesis. Polypeptides containing polyQ-tracts of lengths associated with neurodegenerative diseases compromise membrane trafficking in fast axonal transport. Pathogenic forms of different recombinant constructs for huntingtin and androgen re-

Table 1. Expansion of Polyglutamine Tracts Affects Cell Morphology

Cell Line	wtAR	902-6	902-13	wtAR	902-6	wtAR	902-6
Substrate	Collagen	Collagen	Collagen	p-D-lysine	p-D-lysine	Collagen	Collagen
Measured	Tubulin	Tubulin	Tubulin	Tubulin	Tubulin	Cell-Track	Cell-Track
Mean (SEM)	75 (4)	56 (2)	62 (2)	79 (3)	60 (2)	95 (4)	69 (2)
Minimum	39	32	24	32	30	37	38
Median	73	52	61	74	55	81	67
Maximum	138	100	135	179	112	215	194
Sample size	43	96	77	101	101	106	106

902-6 and 902-13 cells (56Q) have shorter processes than wtAR cells (Q20). Cell length was measured in microns in images of fixed cultures stained with tubulin or Cell-Track. Cells were grown on either collagen I- or poly-D-lysine-coated slides. 902-6 cell lengths differed significantly from wtAR cells ($p < 8E-09$ for each sample pair, in Student's t test). 902-13 cell lengths also differed significantly from both wtAR cells and 902-6 cells ($p < 1E-03$ for each sample pair), showing that 902-13 has an intermediate morphological phenotype. Length measurements with Cell-Track were significantly larger than with tubulin for all cases, but the cell length differences between poly-D-lysine and collagen I were not different.

ceptor exhibited a characteristic inhibition of anterograde and retrograde transport distinct from effects seen with a wide range of mutant and normal proteins introduced into isolated axoplasm (Pfister et al., 1989; Ratner et al., 1998; Stenoien and Brady, 1997). This suggests that expansion of polyQ sequences confers a toxic gain of function consistent with dominant inheritance of polyQ diseases. Furthermore, toxic effects of expanded polyQ segments did not require formation of morphologically detectable aggregates.

Characteristic features of polyQ expansion diseases should be explained by any candidate pathogenic mechanism. These include toxic gain of function, threshold polyQ length, preferential loss of neurons, and delayed disease onset (Gusella and MacDonald, 2000; Orr, 2001; Zoghbi and Orr, 2000). Pathological activities gained by expanding polyQ tracts need not be related to normal functions of the various unrelated proteins associated with polyQ neurodegenerative disorders (Fischbeck, 2001).

Axoplasm experiments indicate that polypeptides containing expanded polyQ tracts in cytoplasm are sufficient to affect transport, because isolated axoplasm contains neither nuclei nor protein synthesis. Inhibition of fast axonal transport by peptides containing expanded polyQ tracts occurs at concentrations two orders of magnitude lower than concentrations of motor proteins responsible for transport. Consistent with observations of increased toxicity for truncated polyglutamine proteins (Hackam et al., 1998; Merry et al., 1998; Orr, 2001; Wellington et al., 1998), truncated polypeptides containing expanded polyQ sequences affect transport more severely than full-length proteins, and higher levels of cytoplasmic expanded polyQ tract may be more toxic. These results suggest that proteins with polyQ expansion affect cellular activities dependent on kinesin and dynein, specifically fast axonal transport.

A variety of experiments indicate that neurite outgrowth is dependent on microtubule-based motor proteins. Inhibition of kinesin function with specific antibodies or reduction of kinesin levels with antisense RNA (Amaratunga et al., 1993; Feiguin et al., 1994) inhibits process formation in neurons, indicating a role for kinesin-dependent transport. Similarly, disruption of dynein function inhibits process formation (Ferhat et al., 2001; Hafezparast et al., 2003). Although process formation is a complex, multistep event, inhibition of either kinesin and dynein function is sufficient to inhibit neurite growth. Given that studies in isolated axoplasm exhibit inhibition of both kinesin- and dynein-based vesicle transport by proteins with expanded polyQ tracts, attenuation of process formation by mutant AR polypeptides is consistent with inhibition of kinesin and dynein function by these proteins.

Inhibition of fast axonal transport by pathogenic forms of huntingtin and AR represents a toxic gain of function consistent with dominant inheritance patterns for HD and SBMA. The large size and distinctive subcellular organization of neurons makes them uniquely dependent on fast axonal transport to provide membrane proteins and organelles. Virtually all protein synthesis occurs in perikarya, and materials must be delivered efficiently to axonal regions that may comprise >99.9% of membranes in a neuron (Brady, 1993). Neurons are affected earlier and more severely than other cell types by toxic treatments that compromise fast axonal transport, such as vincristine and acrylamide (Sahenk et al., 1986; Sickles et al., 1996).

Recent reports indicate that inhibition of one or more microtubule-based motors can lead to neurodegeneration. For example, a form of autosomal dominant hereditary spastic paraplegia results from loss of function mutation in the motor domain of a neuron-specific kinesin. Patients with these mutations exhibit axonal degeneration in the longest CNS axons with age of onset between 11 and 30 years of age (Reid et al., 2002). Mutations in another kinesin family member are responsible for Charcot-Marie-Tooth Type 2A peripheral neuropathy (Zhao et al., 2001), indicating that insufficient transport of vesicle proteins can produce degeneration in a subset of neurons. Mutations in dynein also produce motor neuron degeneration (Hafezparast et al., 2003).

The late onset of disease typical of polyQ disorders suggests a chronic rather than acute pathogenic process. Many cellular activities gradually decline during aging, and axonal transport in neurons is no exception. In particular, rates and amounts of material in axonal transport decline with aging (Goemaere-Vanneste et al., 1988; McQuarrie et al., 1989), and these changes correlate with reduced neuronal plasticity and regeneration (Pestronk et al., 1980; Schwab, 1996). Although not examined here, slow axonal transport of the cytoskeleton

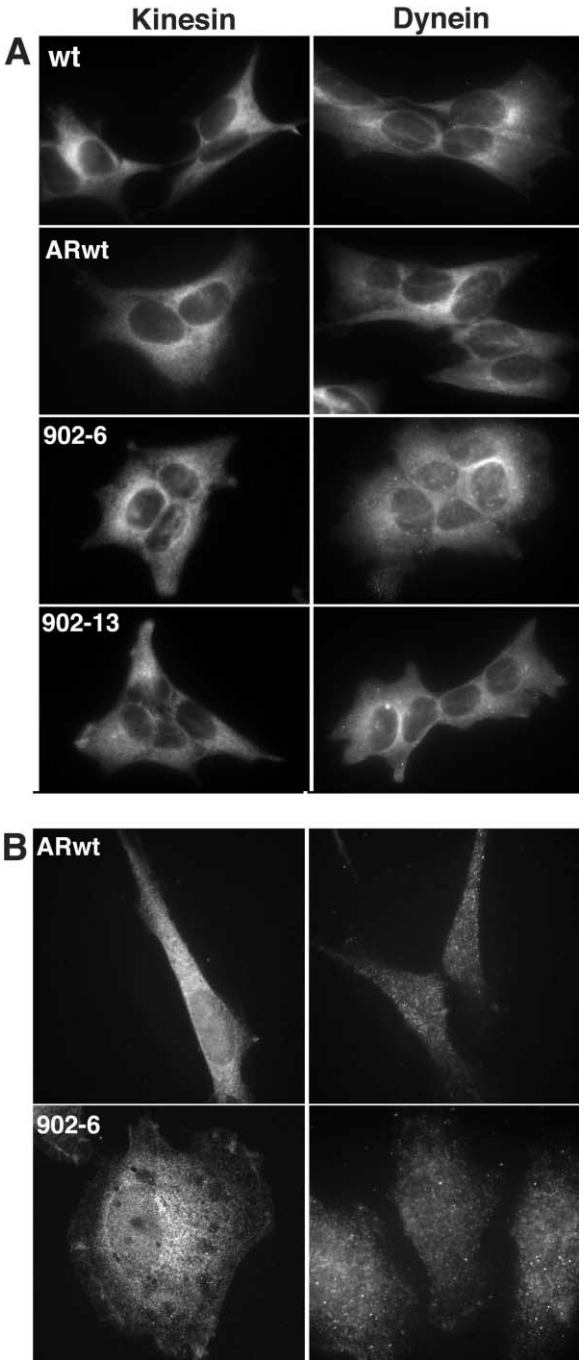

Figure 4. Distributions of Kinesin and Dynein in wtAR and 902-6 Cells

(A) Immunostaining with kinesin antibodies H2 and 63-90 (kinesin) and anti-dynein intermediate chain antibody 74.1 (dynein) in non-transfected cells (wt), cells stably transfected with wild-type AR (wtAR), or cells transfected with mutant AR (902-6 and 902-13) in uninduced cells grown in serum. Localization of kinesin and dynein were similar in all cell lines.

(B) Immunostaining with kinesin and dynein antibodies in wtAR and 902-6 cells induced by BDNF. H2 staining patterns in induced 902-6 cells often appeared patchy with accumulations at the periphery, but such patterns were not seen in wtAR. Similarly, no consistent changes were detected in dynein distribution in 902-6 cells as compared to wtAR cells, although comparisons are difficult due to different cell morphologies of induced wtAR and 902-6 cells.

may also involve kinesins or dynein (Brady, 2000), and inhibition of slow transport could further compromise affected neurons. Presence of pathogenic polyQ polypeptides may compromise fast axonal transport in affected neurons by reducing transport below normal levels for a given age and neuron. When amounts of essential materials delivered by fast transport fall below minimum levels needed, affected neurons begin to die. Thus, inhibition of fast axonal transport by polypeptides containing expanded polyQ segments provides an explanation consistent with a toxic gain of function, preferential loss of neurons, and late disease onset.

Loss of specific neuronal populations is not explicitly addressed by these experiments. However, huntingtin and AR levels vary among neuronal populations, and the specific protein context may determine selective vulnerability of specific neuronal populations (Gusella and MacDonald, 2000; Orr, 2001; Zoghbi and Orr, 2000). Inhibition of transport by subnanomolar concentrations of polypeptides with expanded polyQ tracts suggests an effect on enzymatic activities that modulate fast axonal transport (Morfini et al., 2002; Ratner et al., 1998; Tsai et al., 2000) rather than a direct effect on motor proteins. Cell-specific differences in these essential pathways may lead to lower thresholds for some neuronal populations than others. For example, limiting levels of neurotrophins supplied by neuronal targets may increase vulnerability in a given neuronal population, or there may be differences in ratios of pathogenic polypeptide to neuronal target proteins. Similar arguments were invoked to explain why the largest and/or longest neurons are particularly vulnerable in toxic neuropathies and models of amyotrophic lateral sclerosis (Brady, 1995).

Kinesin- and dynein-based motility of membrane bounded organelles is highly conserved across species. Inhibition of fast axonal transport in isolated axoplasm and of neurite extension in mammalian neuronal cell lines by polypeptides containing pathogenic polyglutamine expansions are consistent with a common mechanism. Ideally, these studies will be extended to transgenic mouse models for glutamine expansion diseases. However, misexpression of proteins, particularly overexpression, may produce pathologies distinct from the polyglutamine expansion pathway (i.e., see Szebenyi et al., 2002). Late onset for neuronal degeneration in polyglutamine expansion diseases suggests that transport defects may be subtle prior to onset of symptoms, particularly in neurons slow to exhibit pathology. Based on observations presented here, we expect the amount of kinesin- and/or dynein-transported cargos in the terminals to be affected and average transport rates to be reduced but not eliminated. Fast axonal transport rates and amounts are not easily measured in the cortical neurons most severely affected in Huntington's disease and SBMA, but a detailed analysis in appropriate neuronal systems should reveal decrements in transport. Precedent for this is found in demonstrations that mutations in presenilin 1 associated with familial forms of Alzheimer's disease increase levels of active glycogen synthase kinase 3 and reduce kinesin-based motility in neurons by 20%–30% (Pigino et al., 2003).

Although polyglutamine expansion diseases share many features, there are also indications that disease-specific elements that may be related to protein context

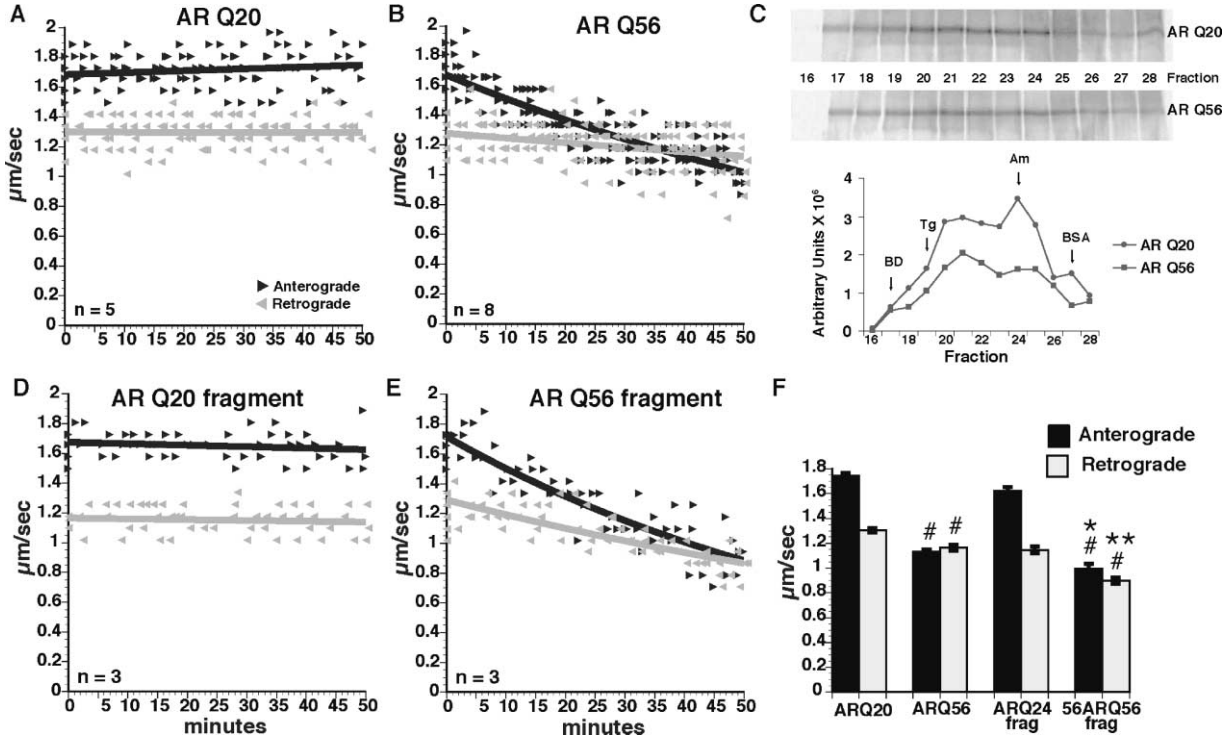

Figure 5. Full-Length and N-Terminal Fragments of Androgen Receptor with Pathogenic PolyQ Domains Inhibit Fast Axonal Transport in Isolated Axoplasm

Full-length or N-terminal fragments of androgen receptor containing wild-type (AR Q20) or pathogenic polyQ (AR-Q56) domains were synthesized by in vitro translation.

(A and B) Full-length AR-Q20 (A) had no effect on transport of organelles in either direction, but AR-Q56 (B) inhibited both directions significantly ($p \leq 0.0001$, pooled t test). The effect of full-length AR-Q56 was more pronounced on anterograde.

(C) Pathogenic and wild-type androgen receptors used in axoplasm experiments behaved indistinguishably in gel filtration chromatography. Neither had detectable levels of aggregated AR, indicating that aggregates were not required for effects on transport.

(D and E) N-terminal truncated AR containing wild-type (AR-Q20 fragment) or pathogenic polyQ (AR-Q56 fragment) tracts were used to determine whether polyQ-containing fragments differed from full-length AR. As with full-length AR, AR-Q20 fragments (D) had no discernible effect on transport, but pathogenic AR-Q56 fragments (E) inhibited both directions of transport.

(F) Histograms comparing actions of normal and pathogenic AR polypeptides on fast axonal transport after 25–35 min of observation. Fast axonal transport with nonpathogenic full-length and N-terminal fragment polypeptides was indistinguishable from vector controls (data not shown). In contrast, pathogenic full-length and N-terminal fragments inhibited fast axonal transport in both directions significantly (#$p \leq 0.0001$ in a pooled t test) relative to corresponding nonpathogenic constructs. Pathogenic N-terminal AR-Q56 fragments inhibited transport to a greater extent than full-length AR-Q56 (*$p \leq 0.0005$ and **$p \leq 0.0001$, pooled t test). As in transfected SH-SY5Y cells, truncated forms of proteins with pathogenic polyQ domains appear more toxic.

or physiological function of polypeptides containing polyglutamine expansions (Gusella and MacDonald, 2000; Orr, 2001). For example, recent reports find that hormonal ligand may play an important role in SBMA (Katsuno et al., 2002; Takeyama et al., 2002). These studies report that increased hormone levels lead to loss of neurons in mice and *Drosophila* models, presumably by increasing nuclear levels of mutant protein. Katsuno et al. (2002) suggest that hormone is required for neuropathology, but this conclusion must be tempered by other observations. For example, Takeyama et al. (2002) note that presence of a truncated form of the AR induces similar pathology without hormone, consistent with our observation that a truncated AR peptide has a more profound effect on axonal transport than full-length receptor. Others have reported that testosterone treatment increases cell viability in cellular models of SBMA (Piccioni et al., 2001). Katsuno et al. (2002) also restricted analysis to relatively young animals (≤30-week-old mice), but neuropathology may occur in the absence of hormone with a longer time course. Consistent with this, many patients with SBMA exhibit signs and symptoms indicative of mild androgen insensitivity (Wieacker et al., 1998), indicating that the expanded repeat AR is not fully competent as a transcription factor. In this context, increasing mutant protein concentration in cell bodies by hormone treatment may enhance toxicity by interfering with transport in the perikarya or by expressing a second cytotoxic effect in the nucleus or both. Regardless, our observations demonstrate that two unrelated sets of polypeptides with polyQ expansions inhibit fast axonal transport.

Effects of N-terminal huntingtin and AR with expanded polyQ tracts on fast axonal transport suggest that decrements in axonal transport are a component of pathogenesis in HD, SBMA, and probably other polyQ expansion diseases. Other neuronal functions may also be compromised in these diseases as a consequence of polyQ

expansion. For example, formation of aggregates and nuclear localization might exacerbate or contribute to neuropathology in these diseases. However, compromised fast axonal transport is likely to be a primary lesion leading to neuronal degeneration, and fast axonal transport represents a promising target for designing and testing treatments to slow or block neurodegeneration.

Experimental Procedures

Recombinant Huntingtin and Androgen Receptor Polypeptides

Expression vectors encoding amino acids 1–548 of human huntingtin protein engineered to contain either an N-terminal FLAG epitope tag or a C-terminal GFP tag were constructed in pCDNA3 (Invitrogen) as described previously (Faber et al., 1998). Plasmids containing full-length or saul amino-terminal fragment androgen receptor constructs were similarly prepared. Polypeptides for these assays were produced by in vitro transcription/translation (Promega; TnT T7 coupled Reticulocyte Lysate system) according to manufacturer's protocols. Typically, 1 μg of plasmid was transcribed in 50 μl reaction mix. To assess protein levels, parallel transcription/translation reactions were performed incorporating ^{35}S-labeled methionine (Amersham) or by quantitative immunoblots. Concentrations were typically between 0.2 and 0.5 nM protein. Generally, higher numbers of glutamines resulted in slightly lower concentrations of translated protein under identical conditions. In vitro translation products were briefly centrifuged to eliminate translation machinery and supernatants frozen in liquid N_2 until used.

In some experiments, androgen receptor translation mixtures were fractionated on Sephacryl S-300 HR. Immunoreactive AR (above) was detected in immunoblots using antibody directed at the N terminus of AR (U402). Relative levels of immunoreactive AR in different column fractions were plotted and compared to elution patterns of molecular size markers (BD: blue dextran dye, 2×10^6 kD; TG: thyroglobulin, 6.69×10^5 kD; Am: amylase, 2×10^5 kD; BSA: bovine serum albumin, 6.6×10^4 kD).

Fast Axonal Transport in Isolated Axoplasm

Axoplasm was extruded from giant axons of squid (*Loligo pealii*; Marine Biological Laboratory, Woods Hole, MA) as described previously (Brady et al., 1985). Briefly, 2–2.5 cm of axon was dissected and 4–5 μl of axoplasm extruded onto a 0 thickness coverslip as a well-organized cytoplasmic cylinder with known polarity. Axoplasm is sandwiched between two coverslips with ≈150 μm thick spacers to form an incubation chamber of 25 μl for perfusion with physiological buffers containing polypeptides of interest. Absence of permeability barriers allows introduction of impermeant compounds like nucleotide analogs (Lasek and Brady, 1985), antibodies (Stenoien and Brady, 1997), and recombinant proteins (Ratner et al., 1998) into axoplasm at defined concentrations. Proteins for perfusion into axoplasm were diluted 1:1 with buffer X (350 mM potassium aspartate, 130 mM taurine, 70 mM betaine, 50 mM glycine, 20 mM HEPES, 13 mM $MgCl_2$, 10 mM EGTA, 3 mM $CaCl_2$, 1 mM glucose [pH 7.2], supplemented with 10 mM ATP), which is modeled after the small molecular weight composition of axoplasm (Brady et al., 1985). Fast axonal transport in isolated axoplasm continues for >2 hr in buffer X or half-strength buffer X (X/2) (Stenoien and Brady, 1997). Recombinant polypeptides were thawed just prior to use and analyzed within 24 hr of thawing. Recombinant polypeptide in X/2 (20 μl) is perfused into the chamber. Small molecular weight components like ATP or amino acids equilibrate between axoplasm and buffer within 2–3 min, whereas polypeptides of the size employed here equilibrate in 10–20 min (Brady et al., 1985).

Fast transport was evaluated by video enhanced contrast, differential interference contrast microscopy using a 100×, 1.3NA planapochromatic objective on a Zeiss Axiomat (Carl Zeiss, Inc., Thornwood, NY) interfaced with a Hamamatsu Argus 20 image processor. Velocities are measured in real time using a Hamamatsu C2117 Videomanipulator. Data was plotted and curves fitted using Deltagraph software (DeltaPoint, Monterrey, CA). Statistical significance was evaluated by Student's or pooled t test of μ1-μ2 using DataDesk 5.0 (Data Description, Ithaca, NY).

SH-SY5Y Cell Culture

Androgen receptor (AR) constructs containing wild-type Q20 and pathogenic (SBMA) Q56 tracts were prepared and stably transfected into SH-SY5Y human neuroblastoma cells (unpublished results). Stably transfected clones of SH-SY5Y cells (wtAR, 902-6, and 902-13) as well as nontransfected cells were grown and differentiated according to Encinas et al. (2000), with some modifications. Two stably transfected mutant cell lines were selected because they expressed comparable levels of full-length androgen receptor, and 902-6 cells expressed a truncated N-terminal fragment of the androgen receptor that accumulated in the cytoplasm. Briefly, cells were plated on poly-D-lysine or collagen surfaces in growth medium (DMEM/F12 medium [GIBCO] supplemented with 10% fetal bovine serum [Hyclone], 2 mM L-glutamine, and a cocktail of antibiotics [Cellgro]). For immunocytochemistry and morphometric studies, cells were plated at densities of 3000–5000 cells/cm^2 on 4-well tissue-tech chamber slides (Becton-Dickinson) and for biochemical studies at 10,000 cells/cm^2 on 10 cm tissue culture dishes. Undifferentiated cells were maintained in growth medium. To induce neuronal differentiation, 10 mM retinoic acid was added in growth medium, typically within 48 hr of cell plating. After 5–7 days of retinoic acid treatment, cells were washed 3 times with serum-free DMEM/F12 and incubated in differentiating medium (DMEM/F12 supplemented with 50 ng/ml BDNF [Alomone], 2 mM L-glutamine, and antibiotics). Cells were maintained in differentiating medium for up to 30 days, with 50% of medium changed every 3–4 days.

Cell Fractionation and Western Blotting

Cells were rinsed with PHEM (60 mM PIPES, 25 mM HEPES, 10 mM EGTA, 1 mM $MgCl_2$ [pH 7.4]) at 37°C, scraped into Homogenization buffer (10 mM HEPES [pH 7.4] and 2 mM EDTA), and homogenized with 20 strokes in a Dounce homogenizer. After 20 min incubation, sucrose was added to a final concentration of 250 mM. Crude nuclear pellet was obtained by centrifugation at 2000 × g for 5 min. Supernatants were further centrifuged at 12,500 × g for 8 min to obtain a mitochondrial fraction, and that supernatant was centrifuged at 150,000 × g for 40 min in a TLA 100.3 rotor to obtain microsomal pellet and cytosolic supernatant fractions. To solubilize samples, SDS was added to 0.1%.

Protein concentrations were determined by Coomassie Plus Protein Assay (Pierce, Rockford, IL). All samples were brought to the same concentration in homogenization buffer and sample buffer (0.35 M Tris-HCl [pH 6.8], 10.3% SDS [Pierce], 36% glycerol, 5% β-mercaptoethanol, 0.01% bromphenol blue), and equal amounts of protein from each sample were loaded to lanes of a 4%–15% SDS-PAGE gel. Some gels were Coomassie blue stained to further assure similar protein concentrations in all the samples. Proteins were transferred to nitrocellulose (Schleicher & Schuell) for 1 hr at 100 V in Tris-glycine buffer. Transfer of proteins was assessed by Ponceau (Sigma) staining. Membranes were blocked by incubation in 5% non-fat dry milk in PBS [pH 7.4] for 1 hr at 4°C. Antibodies were incubated with membranes in blocking buffer overnight at 4°C. Washes after incubations were in 0.25% Tween-20 in PBS at room temperature and were repeated 5 times, for a total length of about 30 min. Blots were then incubated with secondary antibodies for 1 hr at 4°C, then washed as above, except last washes were without detergent. Finally, blots were developed in an ECL chemiluminescent assay (Amersham Biosciences) and exposed to Blue Biofilm (Denville Scientific) for 30 s–30 min. For quantitation, immunoblots were done under identical conditions and AR immunoreactivity visualized by chemiluminescence. Exposures were adjusted to assure that no band was saturated in scanned films. Band density was quantified with ImageJ software (NIH) and pixel values normalized to a loading control.

Immunofluorescence

Cells were rinsed with PHEM at 37°C, fixed in 2% paraformaldehyde (Fisher)/0.01% glutaraldehyde (Electron Microscopy Sciences) in PHEM for 10 min at 37°C, and rinsed several times in cold PBS (pH 7.4) or fixed in cold methanol for 10 min. Aldehyde-fixed cells were

permeabilized in 0.2% triton X-100 in PBS for 10 min at room temperature. Nonspecific binding was blocked by incubation in 2.5% gelatin/3% BSA/0.2% Tween 20 in PBS (pH 7.4) for ≥1 hr. Antibodies were diluted in blocking solution and incubated on slides overnight at 4°C. Kinesin was detected with H2 and 63–90 antibodies; dynein with anti 74.1 (Pfister et al., 1996); tubulin with DM1A (Sigma); androgen receptor with N20 (Santa Cruz), 447 (Santa Cruz), U402, and U407 (McPhaul); and polyglutamine with 1C2 (Chemicon). Washes were in 0.2% Tween-20 in PBS. Goat anti-mouse and anti-rabbit secondary antibodies, labeled with Texas red, Alexa 488, or Alexa 594 (Molecular Probes), were applied at room temperature for 1 hr and slides washed as above. To stain nuclei, slides were dipped into 0.5 μg/ml Hoechst solution (Aldrich Chemicals, St. Louis, MO) for 2–10 min. After rinses in 50 mM Tris (pH 8.0), sections were coverslipped with Gel/Mount (Biomedia, Foster City, CA).

Axoplasms were extruded onto coverslips and incubated with 5 μl of HD548 Q23flag, or HD548 Q62flag in X/2 to minimize dilution or extraction. Samples were incubated for 30 min at room temperature, and then 15 μl of HBS (50 mM HEPES [pH 7.2], 150 mM NaCl) + 2% bovine serum albumin (BSA) was added to minimize nonspecific interactions. Excess buffer was wicked off and the process repeated. Axoplasms were then fixed by immersion either in 95% ethanol/5% acetic acid at −20°C for 10 min or in 50 μl freshly prepared 3.7% paraformaldehyde in HBS at room temperature for 30 min, replacing formaldehyde fix 3–4 times during fixation. After fixation, axoplasms were rinsed once in 50 μl HBS and once in 50 μl HBS + 2% BSA at room temperature for 10 min each wash. Axoplasms were incubated for 1 hr at room temperature in 50 μl anti-FLAG antibody (M2 or M5 monoclonal antibodies, Eastman Kodak) made up at 20 μg/ml in HBS + 10% BSA. Samples were washed 3 times as above in HBS + 2% BSA, then incubated with TRITC-goat antimouse IgG (Jackson ImmunoResearch) at 30 μg/ml in HBS + 10% BSA for 1 hr at room temperature. Finally, samples were washed 3 times again in HBS + 2% BSA. Slides were mounted with Slow Fade Light (Molecular Probes) and sealed. Images were obtained using a Zeiss LSM 410 Laser Scanning Confocal Microscope. All images were acquired with identical settings and the panel assembled in Photoshop before adjusting contrast on both panels at the same time.

Cell Imaging and Morphometry

Stained preparations were viewed with epifluorescent illumination using AttoArc on a Zeiss Axiovert 100M microscope (Thornwood, NY). Objectives used included 40× F Fluar (NA 1.3) and 100× (NA 1.4) Plan Apochromat. Images were obtained with an Orca CCD camera (Hamamatsu, Japan) controlled by Openlab (Improvision, Boston, MA) and prepared for presentation in Photoshop (Adobe Systems, Mountain View, CA). Images within a panel were adjusted together for contrast. Live cells were imaged by phase optics and images acquired on the same imaging platform. Morphometric measurements were done in Openlab. Statistical significance for differences in cell number and lengths were evaluated by Student's t test in Microsoft Excel and in Deltagraph and additional statistical tests with DataDesk software.

Acknowledgments

Research was supported by NINDS grants NS23868, NS23320, NS41170, and NS43408 to S.T.B.; NINDS grants NS16367 (HD Center Without Walls) and NS32765 to M.E.M.; and NIDDK grant DK03892 and Welch grant I-1090 to M.J.M. P.W.F. was a fellow of the Human Frontiers Program. The authors wish to thank Shelley Sheridan and Huichuan Reyna for technical assistance. We also wish to express our gratitude to Donald Price for his thoughtful comments.

Received: March 11, 2003
Revised: June 23, 2003
Accepted: August 25, 2003
Published: September 24, 2003

References

Amaratunga, A., Morin, P., Kosik, K., and Fine, R. (1993). Inhibition of kinesin synthesis and rapid anterograde axonal transport in vivo by antisense oligonucleotide. J. Biol. Chem. *268*, 17427–17430.

Block-Galarza, J., Chase, K.O., Sapp, E., Vaughn, K.T., Vallee, R.B., DiFiglia, M., and Aronin, N. (1997). Fast transport and retrograde movement of huntingtin and HAP 1 in axons. Neuroreport *8*, 2247–2251.

Brady, S.T. (1993). Axonal dynamics and regeneration. In Neuroregeneration, A. Gorio, ed. (New York: Raven Press), pp. 7–36.

Brady, S.T. (1995). Motor neuron diseases: interfering with the runners. Nature *375*, 12–13.

Brady, S.T. (2000). Neurofilaments run sprints not marathons. Nat. Cell Biol. *2*, E43–E45.

Brady, S.T., Lasek, R.J., and Allen, R.D. (1985). Video microscopy of fast axonal transport in isolated axoplasm: a new model for study of molecular mechanisms. Cell Motil. *5*, 81–101.

Brady, S.T., Pfister, K.K., and Bloom, G.S. (1990). A monoclonal antibody against kinesin inhibits both anterograde and retrograde fast axonal transport in squid axoplasm. Proc. Natl. Acad. Sci. USA *87*, 1061–1065.

Chen, H.K., Fernandez-Funez, P., Acevedo, S.F., Lam, Y.C., Kaytor, M.D., Fernandez, M.H., Aitken, A., Skoulakis, E.M., Orr, H.T., Botas, J., and Zoghbi, H.Y. (2003). Interaction of akt-phosphorylated ataxin-1 with 14-3-3 mediates neurodegeneration in spinocerebellar ataxia type 1. Cell *113*, 457–468.

DiFiglia, M., Sapp, E., Chase, K., Schwarz, C., Meloni, A., Young, C., Martin, E., Vonsattel, J.P., Carraway, R., Reeves, S.A., et al. (1995). Huntingtin is a cytoplasmic protein associated with vesicles in human and rat brain neurons. Neuron *14*, 1075–1081.

Elluru, R., Bloom, G.S., and Brady, S.T. (1995). Fast axonal transport of kinesin in the rat visual system: functionality of the kinesin heavy chain isoforms. Mol. Biol. Cell *6*, 21–40.

Emamian, E.S., Kaytor, M.D., Duvick, L.A., Zu, T., Tousey, S.K., Zoghbi, H.Y., Clark, H.B., and Orr, H.T. (2003). Serine 776 of ataxin-1 is critical for polyglutamine-induced disease in SCA1 transgenic mice. Neuron *38*, 375–387.

Encinas, M., Iglesias, M., Liu, Y., Wang, H., Muhaisen, A., Cena, V., Gallego, C., and Comella, J.X. (2000). Sequential treatment of SH-SY5Y cells with retinoic acid and brain-derived neurotrophic factor gives rise to fully differentiated, neurotrophic factor-dependent, human neuron-like cells. J. Neurochem. *75*, 991–1003.

Faber, P.W., Barnes, G.T., Srinidhi, J., Chen, J., Gusella, J.F., and MacDonald, M.E. (1998). Huntingtin interacts with a family of WW domain proteins. Hum. Mol. Genet. *7*, 1463–1474.

Feiguin, F., Ferreira, A., Kosik, K.S., and Caceres, A. (1994). Kinesin-mediated organelle translocation revealed by specific cellular manipulations. J. Cell Biol. *127*, 1021–1039.

Ferhat, L., Rami, G., Medina, I., Ben-Ari, Y., and Represa, A. (2001). Process formation results from the imbalance between motor-mediated forces. J. Cell Sci. *114*, 3899–3904.

Fischbeck, K.H. (2001). Polyglutamine expansion neurodegenerative disease. Brain Res. Bull. *56*, 161–163.

Goemaere-Vanneste, J., Courad, J.-Y., Hassig, R., Di Giamberardino, L., and van den Bosch de Aguilar, P. (1988). Reduced axonal transport of the G4 molecular form of acetylcholinesterase in the rat sciatic nerve during aging. J. Neurochem. *51*, 1746–1754.

Grierson, A.J., Shaw, C.E., and Miller, C.C. (2001). Androgen induced cell death in SHSY5Y neuroblastoma cells expressing wild-type and spinal bulbar muscular atrophy mutant androgen receptors. Biochim. Biophys. Acta *1536*, 13–20.

Gusella, J.F., and MacDonald, M.E. (2000). Molecular genetics: unmasking polyglutamine triggers in neurodegenerative disease. Nat. Rev. Neurosci. *1*, 109–115.

Hackam, A.S., Singaraja, R., Wellington, C.L., Metzler, M., McCutcheon, K., Zhang, T., Kalchman, M., and Hayden, M.R. (1998). The influence of huntingtin protein size on nuclear localization and cellular toxicity. J. Cell Biol. *141*, 1097–1105.

Hafezparast, M., Klocke, R., Ruhrberg, C., Marquardt, A., Ahmad-Annuar, A., Bowen, S., Lalli, G., Witherden, A.S., Hummerich, H., Nicholson, S., et al. (2003). Mutations in dynein link motor neuron degeneration to defects in retrograde transport. Science *300*, 808–812.

Hughes, R.E., and Olson, J.M. (2001). Therapeutic opportunities in polyglutamine disease. Nat. Med. *7*, 419–423.

Huynh, D.P., Figueroa, K., Hoang, N., and Pulst, S.M. (2000). Nuclear localization or inclusion body formation of ataxin-2 are not necessary for SCA2 pathogenesis in mouse or human. Nat. Genet. *26*, 44–50.

Katsuno, M., Adachi, H., Kume, A., Li, M., Nakagomi, Y., Niwa, H., Sang, C., Kobayashi, Y., Doyu, M., and Sobue, G. (2002). Testosterone reduction prevents phenotypic expression in a transgenic mouse model of spinal and bulbar muscular atrophy. Neuron *35*, 843–854.

Lasek, R.J., and Brady, S.T. (1985). Attachment of transported vesicles to microtubules in axoplasm is facilitated by AMP-PNP. Nature *316*, 645–647.

Li, J.-Y., Pfister, K.K., Brady, S.T., and Dahlström, A. (2000). Cytoplasmic dynein conversion at a crush injury in rat peripheral axons. J. Neurosci. Res. *61*, 151–161.

McQuarrie, I.G., Brady, S.T., and Lasek, R.J. (1989). Retardation in axonal transport of cytoskeletal elements during maturation and aging. Neurobiol. Aging *10*, 359–365.

Merry, D.E., Kobayashi, Y., Bailey, C.K., Taye, A.A., and Fischbeck, K.H. (1998). Cleavage, aggregation and toxicity of the expanded androgen receptor in spinal and bulbar muscular atrophy. Hum. Mol. Genet. *7*, 693–701.

Morfini, G., Szebenyi, G., Elluru, R., Ratner, N., and Brady, S.T. (2002). Glycogen synthase kinase 3 phosphorylates kinesin light chains and negatively regulates kinesin-based motility. EMBO J. *23*, 281–293.

Morris, J., and Lasek, R.J. (1984). Monomer-polymer equilibria in the axon: direct measurement of tubulin and actin as polymer and monomer in axoplasm. J. Cell Biol. *98*, 2064–2076.

Ordway, J.M., Tallaksen-Greene, S., Gutekunst, C.A., Bernstein, E.M., Cearley, J.A., Wiener, H.W., Dure, L.S. 4th, Lindsey, R., Hersch, S.M., Jope, R.S., et al. (1997). Ectopically expressed CAG repeats cause intranuclear inclusions and a progressive late onset neurological phenotype in the mouse. Cell *91*, 753–763.

Orr, H.T. (2001). Beyond the Qs in the polyglutamine diseases. Genes Dev. *15*, 925–932.

Perez, M.K., Paulson, H.L., and Pittman, R.N. (1999). Ataxin-3 with an altered conformation that exposes the polyglutamine domain is associated with the nuclear matrix. Hum. Mol. Genet. *8*, 2377–2385.

Pestronk, A., Drachman, D.B., and Griffin, J.W. (1980). Effects of aging on nerve sprouting and regeneration. Exp. Neurol. *70*, 65–82.

Pfister, K.K., Wagner, M.C., Stenoien, D., Bloom, G.S., and Brady, S.T. (1989). Monoclonal antibodies to kinesin heavy and light chains stain vesicle-like structures, but not microtubules, in cultured cells. J. Cell Biol. *108*, 1453–1463.

Pfister, K.K., Salata, M.W., Dillman, J.F., Vaughan, K.T., Vallee, R.B., Torre, E., and Lye, R.J. (1996). Differential expression and phosphorylation of the 74-kDa intermediate chains of cytoplasmic dynein in cultured neurons and glia. J. Biol. Chem. *271*, 1687–1694.

Piccioni, F., Simeoni, S., Andriola, I., Armatura, E., Bassanini, S., Pozzi, P., and Poletti, A. (2001). Polyglutamine tract expansion of the androgen receptor in a motoneuronal model of spinal and bulbar muscular atrophy. Brain Res. Bull. *56*, 215–220.

Piccioni, F., Pinton, P., Simeoni, S., Pozzi, P., Fascio, U., Vismara, G., Martini, L., Rizzuto, R., and Poletti, A. (2002). Androgen receptor with elongated polyglutamine tract forms aggregates that alter axonal trafficking and mitochondrial distribution in motor neuronal processes. FASEB J. *16*, 1418–1420.

Pigino, G., Morfini, G., Mattson, M.P., Brady, S.T., and Busciglio, J. (2003). Alzheimer's Presenilin 1 mutations impair kinesin-based axonal transport. J. Neurosci. *23*, 4499–4508.

Ratner, N., Bloom, G.S., and Brady, S.T. (1998). A role for cdk5 kinase in fast anterograde axonal transport: novel effects of olomoucine and the APC tumor suppressor protein. J. Neurosci. *18*, 7717–7726.

Reddy, P.H., Williams, M., and Tagle, D.A. (1999). Recent advances in understanding the pathogenesis of Huntington's disease. Trends Neurosci. *22*, 248–255.

Reid, E., Kloos, M., Ashley-Koch, A., Hughes, L., Bevan, S., Svenson, I.K., Graham, F.L., Gaskell, P.C., Dearlove, A., Pericak-Vance, M.A., et al. (2002). A kinesin heavy chain (KIF5A) mutation in hereditary spastic paraplegia (SPG10). Am. J. Hum. Genet. *71*, 1189–1194.

Rubinsztein, D.C. (2002). Lessons from animal models of Huntington's disease. Trends Genet. *18*, 202–209.

Sahenk, Z., Mendell, J., and Brady, S.T. (1986). Studies on the pathogenesis of vincristine-induced neuropathy. Muscle Nerve *10*, 80–84.

Schwab, M.E. (1996). Structural plasticity of the adult CNS. Int. J. Dev. Neurosci. *14*, 379–385.

Sharp, A.H., Loev, S.J., Schilling, G., Li, S.H., Li, X.J., Bao, J., Wagster, M.V., Kotzuk, J.A., Steiner, J.P., Lo, A., et al. (1995). Widespread expression of Huntington's disease gene (IT15) protein product. Neuron *14*, 1065–1074.

Sickles, D.W., Brady, S.T., Testino, A., and Wrenn, R.W. (1996). Direct effect of the neurotoxicant acrylamide on kinesin-based microtubule motility. J. Neurosci. Res. *46*, 7–17.

Stenoien, D.S., and Brady, S.T. (1997). Immunochemical analysis of kinesin light chain function. Mol. Biol. Cell *8*, 675–689.

Szebenyi, G., Smith, G.M., Li, P., and Brady, S.T. (2002). Overexpression of neurofilament H disrupts normal cell structure and function. J. Neurosci. Res. *68*, 185–198.

Takeyama, K., Ito, S., Yamamoto, A., Tanimoto, H., Furutani, T., Kanuka, H., Miura, M., Tabata, T., and Kato, S. (2002). Androgen-dependent neurodegeneration by polyglutamine-expanded human androgen receptor in *Drosophila*. Neuron *35*, 855–864.

Trettel, F., Rigamonti, D., Hilditch-Maguire, P., Wheeler, V.C., Sharp, A.H., Persichetti, F., Cattaneo, E., and MacDonald, M.E. (2000). Dominant phenotypes produced by the HD mutation in STHdh(Q111) striatal cells. Hum. Mol. Genet. *9*, 2799–2809.

Trottier, Y., Devys, D., Imbert, G., Saudou, F., An, I., Lutz, Y., Weber, C., Agid, Y., Hirsch, E.C., and Mandel, J.L. (1995). Cellular localization of the Huntington's disease protein and discrimination of the normal and mutated form. Nat. Genet. *10*, 104–110.

Tsai, M.-Y., Morfini, G., Szebenyi, G., and Brady, S.T. (2000). Modulation of kinesin-vesicle interactions by Hsc70: implications for regulation of fast axonal transport. Mol. Biol. Cell *11*, 2161–2173.

Velier, J., Kim, M., Schwarz, C., Kim, T.W., Sapp, E., Chase, K., Aronin, N., and DiFiglia, M. (1998). Wild-type and mutant huntingtins function in vesicle trafficking in the secretory and endocytic pathways. Exp. Neurol. *152*, 34–40.

Wellington, C.L., Ellerby, L.M., Hackam, A.S., Margolis, R.L., Trifiro, M.A., Singaraja, R., McCutcheon, K., Salvesen, G.S., Propp, S.S., Bromm, M., et al. (1998). Caspase cleavage of gene products associated with triplet expansion disorders generates truncated fragments containing the polyglutamine tract. J. Biol. Chem. *273*, 9158–9167.

Wieacker, P.F., Knoke, I., and Jakubiczka, S. (1998). Clinical and molecular aspects of androgen receptor defects. Exp. Clin. Endocrinol. Diabetes *106*, 446–453.

Zhao, C., Takita, J., Tanaka, Y., Setou, M., Nakagawa, T., Takeda, S., Yang, H.W., Terada, S., Nakata, T., Takei, Y., et al. (2001). Charcot-Marie-Tooth disease type 2A caused by mutation in a microtubule motor KIF1Bbeta. Cell *105*, 587–597.

Zoghbi, H.Y., and Orr, H.T. (2000). Glutamine repeats and neurodegeneration. Annu. Rev. Neurosci. *23*, 217–247.